2014 International Conference on Unmanned Aircraft Systems (ICUAS)
May 27-30, 2014. Orlando, FL, USA

Improving the performance of aerial vehicles with delayed measures via State Predictor-Control: Experimental data validation

A. Alatorre, P. Castillo and S. Mondié

***Abstract*— A state predictor control scheme is presented in this paper. The predictor is based on the Fundamental Calculus Theorem and its stability analysis is proved using the Backstepping approach. The proposed predictor-control scheme is validated in the nonlinear model of a quadrotor vehicle with delayed inputs. In order to prove its robustness in simulation, noise and dropout data are included in the emulation of the closed-loop system. In addition, real-data are also used to validate the predictor-control scheme. Numerical and experimental data results confirm the well behavior of the closed-loop system.**

I. Introduction

Aerial vehicles have a huge field of applications including surveillance operations, weather observation, disaster relief coordination, and civil engineering inspections, and even package delivery. The automatization of the flight of these vehicles is relevant in order to guarantees security or to avoid repetitive tasks.

In some applications the UAV needs to be at hover, because of that VTOLs (Vertical Take Off and Landing) aircrafts are usually used. The quadrotor has become the VTOL configuration most popular among researchers as their aerodynamic characteristics and simple structure turns them into an interesting testbed.

Several control algorithms aiming at the stabilization of these aerial vehicles can be found in the literature [1]-[4]. Some of these control/navigation strategies have been applied in real-time using very efficient but expensive sensing systems [5]. Others research teams use commercial sensors combined with observer/predictor algorithms that improve the measurements [6]. Whatever the case, one common problem when applying the control strategies in real-time is the delay in the measurement that is represented as input delays. When these delays are significant, the performance of the closed-loop system suffers and crash may occur.

level (trajectory design and planning) to the bottom level (stabilization and tracking). Most important is to know the correct states of the vehicle, such as orientation, absolute position, and so on. Most UAVs are equipped with various sensors to correctly measure the state variables. days existe a great variety of sensors with diferente capabilities and characteristics and as we could imagines also there exist high cost and low cost sensors. Several differences could be made between a high price sensor and the cheaper ones, such as precision and speed (rate measurement). Therefore a UAV with good erformances its a high price UAV.

sensor provides unbiased measurements at centimeter level accuracy, and the direct use of GPS avoids complex computations. This approach has been successfully applied to small UAVs. As a result, difficulties arise when one needs the absolute position at higher rates than the rates given by this sensors. cost sensors, to be more prescicely with a GPS and a IMU, and attack one of the biggest problem of this kind of sensor "the delay in the measurements". the vehicle or in many istances desestabilize it.

In the past, the control of linear processes with time delay in either the input or the output have been addressed with strategies such as the Smith Predictor (SP), [7], and the Finite Spectrum Assignment (FSA), [8]. The stabilization of chains of integrators with delayed control has been a difficult topic for researchers due robustness problems respect to the delay values. In [9] and [10] good theoretical solutions are presented, butt realization problems may arrise [11], [12]. For a delayed plant with no modeling error a predictor-based control can achieve a performance that approaches at the delay free system as in [13], [14] and [15]. An overview of contributions on systems with inputs delayed can be found in [17] and [18]. In [19] a predictor scheme that improves the position of the aerial vehicle.

In this work, some ideas of [19] are revisited, improved and expanded to the general case, i.e. a chain of integrators of order n. In addition, a stability analysis is presented following the approach proposed in [17]. Another strong point of this work is the fact that the state predictor is used in all the states of the quadrotor (orientation and position). Recall that when the angular position and rate are delayed it is very difficult (or impossible) to stabilize the helicopter at hover.

The outline of the paper is the following : A brief mathematical background is introduced in section I. The main results, the state predictor and the stability analysis in the linear case, are given in section II. The mathematical representation of the quadrotor vehicle and the control algorithms are described in section III-A. In section IV, the predictor implementation and the numerical validation of the scheme regarding robustness with respect to noise and dropout data are discussed. The validation with real-data is presented in section V. Concluding remarks and future work are given in section VI.

A. Mathematical Background

Theorem 1: (Fundamental Theorem of Calculus.) Let f a

A. Alatorre and S. Mondié are with the CINVESTAV-IPN, Mexico, (e-mail: (aalatorre, smondie)@ctrl.cinvestav.mx)

P. Castillo is with LAFMIA laboratory, UMI 3275, CINVESTAV - IPN, Mexico (e-mail: castillo@hds.utc.fr).

continuous function in the closed interval [a,b], and let g a function such that

$$g'(x) = f(x), \forall x \in [a,b] \tag{1}$$

then

$$\int_a^b f(t)dt = g(b) - g(a) \tag{2}$$

Note : if $x = a$, the derivative in (1) is a hand side derivative, and if $x = b$, the derivative in (1), is a left hand side derivative.

II. State predictor

Proposition 1: Consider the delayed chain of integrators

$$\begin{array}{rcl} \dot{x}_1 &=& x_2 \\ \dot{x}_2 &=& x_3 \\ \vdots &=& \vdots \\ \dot{x}_{n-1} &=& x_n \\ \dot{x}_n &=& u(t-\tau) \end{array} \tag{3}$$

where $u(t-\tau)$ is the control input delayed by τ units of time. The controller

$$u(t) = \mathbf{K}\hat{\mathbf{x}}(t) \tag{4}$$

stabilizes system (3). Here $\mathbf{K}$ is a vector gain that stabilizes the delay free system and $\hat{\mathbf{x}}(t)$ is the predicted state defined as

$$\hat{\boldsymbol{x}}(t) = e^{\tau A}\boldsymbol{x}(t-\tau) + \boldsymbol{\varphi}\big(u(t)\big) \tag{5}$$

where

$$e^{\tau A} = \begin{pmatrix} 1 & \tau & \frac{\tau^2}{2} & \dots & \frac{\tau^{n-1}}{(n-1)!} \\ 0 & 1 & \tau & \dots & \frac{\tau^{n-2}}{(n-2)!} \\ 0 & 0 & 1 & \dots & \frac{\tau^{n-3}}{(n-3)!} \\ \vdots & \vdots & \vdots & \ddots & \vdots \\ 0 & 0 & 0 & \dots & \tau \\ 0 & 0 & 0 & \dots & 1 \end{pmatrix}$$

$$\varphi(u(t)) = \begin{pmatrix} \int_{t-\tau}^{t}\int_{t-\tau}^{t_1}\dots\int_{t-\tau}^{t_{n-1}} u(t_n)dt_n dt_{n-1}\dots dt_1 \\ \int_{t-\tau}^{t}\int_{t-\tau}^{t_1}\dots\int_{t-\tau}^{t_{n-2}} u(t_{n-1})dt_{n-1}dt_{n-2}\dots dt_1 \\ \vdots \\ \int_{t-\tau}^{t}\int_{t-\tau}^{t_1} u(t_2)dt_2dt_1 \\ \int_{t-\tau}^{t} u(t_1)dt_1 \end{pmatrix}$$

Proof: The proof of the proposition takes three steps : First, it is shown that equation (5) holds. Second, system (3) is rewritten using the Backstepping technique. Finally, the stability analysis of the closed-loop system is carried out.

Step 1 : Theorem 1 implies that

$$\int_{t-\tau}^{t} \dot{f}(s)ds = f(t) - f(t-\tau) \tag{6}$$

Applying Theorem 1 to system (3), and algebraic manipulations lead to

$$\begin{array}{rcl} \hat{x}_1(t) &=& x_1(t-\tau) + x_2(t-\tau)\tau + x_3(t-\tau)\frac{\tau^2}{2} \\ && + \dots + x_{n-1}\frac{\tau^{n-2}}{(n-2)!} + x_n\frac{\tau^{n-1}}{(n-1)!} \\ && + \int_{t-\tau}^{t}\int_{t-\tau}^{t_1}\dots\int_{t-\tau}^{t_{n-1}} u(t_n)dt_n dt_{n-1}\dots dt_1 \\ \hat{x}_2(t) &=& x_2(t-\tau) + x_3(t-\tau)\tau + x_4(t-\tau)\frac{\tau^2}{2} \\ && + \dots + x_{n-1}\frac{\tau^{n-3}}{(n-3)!} + x_n\frac{\tau^{n-2}}{(n-2)!} \\ && + \int_{t-\tau}^{t}\int_{t-\tau}^{t_1}\dots\int_{t-\tau}^{t_{n-2}} u(t_{n-1})dt_{n-1}dt_{n-2}\dots dt_1 \\ \vdots &=& \vdots \\ \hat{x}_{n-1}(t) &=& x_{n-1}(t-\tau) + x_n(t-\tau)\tau \\ && + \int_{t-\tau}^{t}\int_{t-\tau}^{t_1} u(t_2)dt_2dt_1 \\ \hat{x}_n(t) &=& x_n(t-\tau) + \int_{t-\tau}^{t} u(t_1)dt_1 \end{array}$$

Finally, (5) is obtained by rewriting the previous equations in vector form.

Step 2 : Consider the following system

$$\dot{x}(t) = Ax(t) + Bu(t-\tau) \tag{7}$$

where $x(t) \in \mathbb{R}^n$, $A \in \mathbb{R}^{n\times n}$, $B \in \mathbb{R}^{n\times p}$ and $u(t-\tau) \in \mathbb{R}^p$. Using the results in [17], the delay in the control input can be modeled by a first-order hyperbolic partial differential equation, also referred to as transport PDE. Thus,

$$\begin{array}{rcl} u_t(s,t) &=& u_s(s,t) \\ u(\tau,t) &=& U(t) \end{array} \tag{8}$$

The solution to this equation is

$$u(s,t) = u(t+s-\tau) \tag{9}$$

and therefore the output

$$u(0,t) = u(t-\tau)$$

gives the delayed input. Hence, system (7) can be written as

$$\dot{x}(t) = Ax(t) + Bu(0,t) \tag{10}$$

The backstepping transformation

$$w(s,t) = u(s,t) - \varphi(u(s,t)) - \Gamma(x(t)) \tag{11}$$

maps the system (8)-(10) into the target system

$$\begin{aligned} \dot{x}(t) &= (A+BK)x(t) + Bw(0,t) \qquad (12)\\ w_t(s,t) &= w_s(s,t)\\ w(\tau,t) &= 0 \end{aligned}$$

This transformation which is defined as

$$(x,u) \longmapsto (x,w)$$

has the lower-triangular form

$$\begin{pmatrix} x \\ w \end{pmatrix} = \begin{pmatrix} I_{n\times n} & 0_{n\times(0,\tau)} \\ \Gamma & \varphi + I_{(0,\tau)\times(0,\tau)} \end{pmatrix} \begin{pmatrix} x \\ u \end{pmatrix} \qquad (13)$$

Here Γ denotes the operator

$$\Gamma : x(t) \longmapsto \Theta(s)x(t)$$

where $\Theta(s)$ is defined as

$$\Theta(s) = \begin{pmatrix} 1 & s & s^2 & \dots & s^{n-1} \\ 0 & 1 & s & \dots & s^{n-2} \\ 0 & 0 & 1 & \dots & s^{n-3} \\ \vdots & \vdots & \vdots & \ddots & \vdots \\ 0 & 0 & 0 & \dots & s \\ 0 & 0 & 0 & \dots & 1 \end{pmatrix}$$

and φ denotes de operator

$$\varphi : u(s,t) \longmapsto \begin{pmatrix} \Lambda \int_0^s \int_0^{s_1} \dots \int_0^{s_{n-1}} u(s_{n,t}) ds_n ds_{n-1} \dots ds_1 \\ \Lambda \int_0^s \int_0^{s_1} \dots \int_0^{s_{n-2}} u(s_{n-1},t) ds_{n-1} ds_{n-2} \dots ds_1 \\ \vdots \\ \Lambda \int_0^s \int_0^{s_1} u(s_2,t) ds_2 ds_1 \\ \Lambda \int_0^s u(s_1,t) ds_1 \end{pmatrix}$$

where Λ is a scalar value that will be defined later.

Computing the time and spatial derivatives of the backstepping transformation (11), yields

$$\begin{aligned} w_s(s,t) &= u_s(s,t) - \Theta'(s)x(t) - \Lambda \int_0^s u(s_n,t) ds_n \\ w_t(s,t) &= u_s(s,t) - \Theta(s)Ax(t) - \Theta(s)Bu(0,t) \\ &- \Lambda \int_0^s u(s_n,t) ds_n + u(0,t)\zeta(s) \end{aligned}$$

where

$$\zeta(s) := \begin{pmatrix} \frac{s^{n-1}}{(n-1)!} \\ \frac{s^{n-2}}{(n-2)!} \\ \vdots \\ s \\ 1 \end{pmatrix} \qquad (14)$$

Subtracting $w_t(s,t) - w_s(s,t) = 0$, gives

$$\begin{aligned} 0 &= \Theta(s)\zeta(s)u(0,t) - \Theta(s)Ax(t) - \Theta(s)Bu(0,t) + \Theta'(s)x(t) \\ 0 &= (\Lambda\zeta(s) - \Theta(s)B)\,u(0,t) + (\Theta'(s) - \Theta(s)A)x(t) \\ 0 &= \Lambda\zeta(s) - \Theta(s)B \qquad (15) \\ 0 &= \Theta'(s) - \Theta(s)A \qquad (16) \end{aligned}$$

the expression (15) is an ordinary differential equation. To find its initial condition, we set $s = 0$ in (11), hence

$$w(0,t) = u(0,t) - \Theta(0)x(t) \qquad (17)$$

Introducing (17) into (12), gives

$$\dot{x}(t) = Ax(t) + Bu(0,t) + B(K - \Theta(0))x(t)$$

Comparing this equation with (10) implies

$$\Theta(0) = K$$

Therefore, the solution of (15) is of the form

$$\Theta(s) = Ke^{As} \qquad (18)$$

From (15),

$$\begin{aligned} \Lambda &= \Theta(s)B\zeta^{-1}(s) \\ &= Ke^{As}B\zeta^{-1}(s) \end{aligned}$$

where $\zeta^{-1}(s)$ denotes the inverse operator. Therefore we have that

$$e^{As}B = \zeta(s)$$

then

$$\Lambda = K$$

Substituting the gains Λ and $\Theta(s)$ into the transformation (11) and setting $s = \tau$, the controller is then given by

$$u(\tau,t) = Ke^{\tau A} + K\varphi(u(\tau,t)) \qquad (19)$$

Step 3 : We now prove that the closed-loop system composed of the plant (8) and (10) with the controller (19) is exponentially stable at the origin in the sense of the norm

$$\left(\|x(t)^2\| + \int_0^\tau u(s,t)^2 ds \right)^{1/2}$$

We first demonstrate that the origin of the target system (12) is exponentially stable. Consider the following Lyapunov-Krasovskii functional

$$V(t) = x(t)^T P x(t) + \frac{a}{2} \int_0^\tau (1+s) w(s,t)^2 ds \qquad (20)$$

where $P = P^T > 0$ is the solution of the Lyapunov equation for some $Q = Q^T > 0$, and $a > 0$. The time derivative of (20) is

$$\dot{V}(t) \leq -x(t)^T Q x(t) + \frac{2}{a}\|x(t)^T PB\|^2 - \frac{a}{2} \int_0^\tau w(s,t)^2 ds$$

Let us choose

$$a = \frac{4\lambda_{max}(PBB^TP)}{\lambda_{min}(Q)}$$

where $\lambda_{\max}$ and $\lambda_{\min}$ are the maximum and the minimum eigenvalues of the corresponding matrices. It follows that

$$\dot{V}(x) \leq -\frac{\lambda_{min}(Q)}{2}\|x(t)\|^2 - \frac{a}{2(1+\tau)} \int_0^\tau (1+s) w(s,t)^2 ds$$

hence

$$\dot{V}(t) \leq -\mu V(t) \tag{21}$$

where

$$\mu := -\min\left\{\frac{\lambda_{min}(Q)}{2\lambda_{max}(P)}, \frac{1}{1+\tau}\right\} \tag{22}$$

Using the Backstepping transformation and its inverse form, we get

$$w(s,t) = u(s,t) - \Lambda \int_0^s u(v,t)dv - \Theta(s)x(t) \tag{23}$$

$$u(s,t) = w(s,t) + \Omega \int_0^s w(v,t)dv + \Phi(s)x(t) \tag{24}$$

The expression (20) implies that

$$\omega_1 \left(||x(t)||^2 + \int_0^\tau w(s,t)^2 ds \right) \leq V(t)$$

$$\omega_2 \left(||x(t)||^2 + \int_0^\tau w(s,t)^2 ds \right) \geq V(t)$$

where

$$\omega_1 = \min\left\{\lambda_{min}(P), \frac{a}{2}\right\}$$

$$\omega_2 = \max\left\{\lambda_{max}(P), \frac{a(1+\tau)}{2}\right\}$$

Furthermore (23) and (24) give

$$\int_0^\tau w(s,t)^2 ds \leq \alpha_1 \int_0^\tau u(s,t)^2 ds + \alpha_2 ||x(t)||^2 \tag{25}$$

$$\int_0^\tau u(s,t)^2 ds \leq \beta_1 \int_0^\tau w(s,t)^2 ds + \beta_2 ||x(t)||^2 \tag{26}$$

where

$$\alpha_1 := 3(1+\tau||\Lambda||)$$
$$\alpha_2 := 3||K\Theta||^2$$
$$\beta_1 := 3(1+\tau||\Omega||)$$
$$\beta_2 := 3||K\Phi||^2$$

Hence we obtain

$$\rho_1 \left(||x(t)||^2 + \int_0^\tau u(s,t)^2 ds \right) \leq ||x(t)||^2 + \int_0^\tau w(s,t)^2 ds \tag{27}$$

$$\rho_2 \left(||x(t)||^2 + \int_0^\tau u(s,t)^2 ds \right) \geq ||x(t)||^2 + \int_0^\tau w(s,t)^2 ds \tag{28}$$

where

$$\rho_1 := \frac{1}{\max\{\beta_1, \beta_2 + 1\}}$$
$$\rho_2 := \max\{\alpha_1, \alpha_2 + 1\}$$

Notice that the inequalities for ρ_i, ω_i for $i = 1, 2$ can be combined. Then, it follows that

$$\rho_1\omega_1 \left(||x(t)||^2 + \int_0^\tau u(x,t)^2 dx \right) \leq V(t)$$

$$\rho_2\omega_2 \left(||x(t)||^2 + \int_0^\tau u(x,t)^2 dx \right) \geq V(t)$$

Finally, combining the above with (21) gives

$$||x(t)||^2 + \int_0^\tau u(x,t)^2 dx \leq \xi(t) \left(||x(0)||^2 + \int_0^\tau w(x,0)^2 dx \right)$$

where

$$\xi(t) = \frac{\rho_2\omega_2}{\rho_1\omega_1} e^{-\mu t}$$

which completes the proof of exponential stability. ■

III. Quadrotor vehicle case study

Next, we apply the results of the previous section to a quadrotor aerial device. First we introduce the model we use, the predictor design and the proposed control law.

A. Mathematical representation of a quadrotor

The quadrotor is a well studied aerial vehicle configuration that can be at hover. Its well known mathematical model can be obtained from the Newton's laws or Euler-Lagrange formulation. For our case study we will use its simplified model.

Feedback control systems data typically travel through communication networks from sensors to controller and from controller to actuators. This transport phenomenon often introduce non negligible delays, either constant, time varying, or random, that can seriously degrade the performance, or even destabilize the closed loop system, if the design does not pay due consideration to the delay. In addition to transmission delay, data packets can be lost, and there may also be a nonzero probability that some observation consists of noise only or the measurements contain missing observations. These phenomena are modeled in the present contribution by delaying the control input τ units of times.

Therefore we consider in this contribution the following model of the quadrotor with input delay [20] :

$$\Omega\ddot{\mathbf{X}} = \mathbf{f}(\theta, \phi, \psi, u_\theta, u_\phi, u_\psi, u) \tag{29}$$

where

$$\ddot{X}^T := \begin{pmatrix} \ddot{x}(t) & \ddot{y}(t) & \ddot{z}(t) & \ddot{\psi}(t) & \ddot{\theta}(t) & \ddot{\phi}(t) \end{pmatrix}$$

$$\Omega := \begin{pmatrix} m & 0 & 0 & 0 & 0 & 0 \\ 0 & m & 0 & 0 & 0 & 0 \\ 0 & 0 & m & 0 & 0 & 0 \\ 0 & 0 & 0 & I_\psi & 0 & 0 \\ 0 & 0 & 0 & 0 & I_\theta & 0 \\ 0 & 0 & 0 & 0 & 0 & I_\phi \end{pmatrix}$$

$$\mathbf{f}(\cdot) := \begin{pmatrix} -u(t-\tau)\sin(\theta(t)) \\ u(t-\tau)\cos(\theta(t))\sin(\theta(t)) \\ u(t-\tau)\cos(\theta(t))\cos(\phi(t)) - mg \\ u_\psi(t-\tau) \\ u_\theta(t-\tau) \\ u_\phi(t-\tau) \end{pmatrix}$$

To further simplify the analysis we set $m = 1$, $I_i = 1$. The states in (29) are the position in the x, y and z axis respectively and the orientation θ, ϕ and ψ (pitch, roll and yaw angles respectively) of the aerial vehicle. The available control inputs are $u_\phi(t-\tau)$, $u_\theta(t-\tau)$, $u_\psi(t-\tau)$ and $u(t-\tau)$, for the roll, pitch and yaw torques and the mains thrust, respectively. To simplify further analysis, from now on

$$\begin{aligned} \theta_1 &= \theta \\ \theta_2 &= \dot{\theta} \end{aligned}$$

It is worthy of mention that in order to stabilize the quadrotor with small angles around the equilibrium, it is possible to use the linearized model and the control law proposed in Proposition 1. However, this strategy is not appropriate as our aim is to control the vehicle subject to lateral or longitudinal displacements. In the following we describe a nonlinear algorithm that stabilizes the quadrotor using saturation functions. It will be shown later that, after a time T, this class of controllers impose a linear behavior to the system, and the control law reduces to the form $Kx(t)$ of Proposition 1.

The following control algorithm have been proposed in [20] to stabilize the quadrotor vehicle at hover without any delays consideration ($h_i = 0$) in the measurement or control input. In this work this result is extended to prove that the control law can be also used to stabilize the quadrotor even in presence of delays. The proposed control law is :

$$\begin{aligned} u(t-\tau) &:= (r_1 + mg)\frac{1}{\cos(\theta_1(t-h_2))\cos(\phi_1(t-h_2))} \\ u_\psi(t-\tau) &:= k_{d_\psi}\psi_2(t-h_2) + k_{p_\psi}(\psi_1(t-h_2) - \psi_{1d}) \\ u_\phi(t-\tau) &:= -\sigma_{\phi_1}(\gamma_1 + \sigma_{\phi_2}(\varrho_1 + \sigma_{\phi_3}(\eta_1 + \sigma_{\phi_4}(\zeta_1)))) \\ u_\theta(t-\tau) &:= -\sigma_{\theta_1}(\gamma_2 + \sigma_{\theta_2}(\varrho_2 + \sigma_{\theta_3}(\eta_2 + \sigma_{\theta_4}(\zeta_2)))) \end{aligned}$$

where

$$\begin{aligned} r_1 &:= k_{d_z} z_2(t-h_1) + k_{p_z}(z_1(t-h_1) - z_{1d}(t-h_1) \\ \gamma_1 &:= \phi_2(t-h_2) \\ \varrho_1 &:= \phi_1(t-h_2) + \phi_2(t-h_2) \\ \eta_1 &:= 2\phi_1(t-h_2) + \phi_2(t-h_2) + \frac{y_2(t-h_1)}{g} \\ \zeta_1 &:= \phi_2(t-h_2) + 3\phi_1(t-h_2) + 3\frac{y_2(t-h_1)}{g} + \frac{y_1(t-h_1)}{g} \\ \gamma_2 &:= \theta_2(t-h_2) \\ \varrho_2 &:= \theta_1(t-h_2) + \theta_2(t-h_2) \\ \eta_2 &:= 2\theta_1(t-h_2) + \theta_2(t-h_2) + \frac{x_2(t-h_1)}{g} \\ \zeta_2 &:= \theta_2(t-h_2) + 3\theta_1(t-h_1) + 3\frac{x_2(t-h_1)}{g} + \frac{x_1(t-h_1)}{g} \end{aligned}$$

where $h_i > 0,\ i = 1, 2$ is the delay due to the measurements.

Notice that the closed-loop system for the altitude (z) and the yaw dynamics (ψ) is the representation for two integrators in cascade with input delay, like system (3). In view of Proposition 1 the we propose the control inputs

$$\begin{aligned} u(t) &:= (r_1(t) + mg)\frac{1}{\cos(\hat{\theta}_1(t))\cos(\hat{\phi}_1(t))} \\ u_\psi(t) &:= k_{d_\psi}\hat{\psi}_2(t) + k_{p_\psi}(\hat{\psi}_1(t) - \psi_{1d}) \end{aligned}$$

with $r_1 := k_{d_z}\hat{z}_2(t) + k_{p_z}(\hat{z}_1(t) - z_{1d}(t))$, and $\hat{\theta}_1, \hat{\phi}_1, \hat{\psi}_2, \hat{\psi}_1$ are predicted values.

B. Predictor Implementation

Due to paper length limitations, the implementation of the state predictor is only presented for the longitudinal dynamics ($\hat{x}$, $\hat{\theta}$), notice that the lateral dynamics ($\hat{y}$, $\hat{\phi}$) is addressed similarly.

From Theorem 1 and using four integrators in cascade, we write

$$\int_{t-\tau}^{t} \dot{x}_4(s)ds = x_4(t) - x_4(t-\tau)$$

then

$$\hat{x}_4(t) = x_4(t-\tau) + \int_{t-\tau}^{t} u(s)ds \tag{30}$$

On the other hand, the equation that define $\hat{x}_3(t)$ is

$$\hat{x}_3(t) = x_3(t-\tau) + x_4(t-\tau)\tau + \int_{t-\tau}^{t}\int_{t-\tau}^{s} u(l)dlds$$

Similarly for $\hat{x}_2(t)$ we have

$$\hat{x}_2(t) = x_2(t-\tau) + x_3(t-\tau)\tau + \int_{t-\tau}^{t}\int_{t-\tau}^{s} x_4(l)dlds$$

notice that x_4 is not available, thus we could substitute this value for $\hat{x}_4$ obtained in (30), then

$$\hat{x}_2(t) = x_2(t-\tau) + x_3(t-\tau)\tau + \int_{t-\tau}^{t}\int_{t-\tau}^{s} \hat{x}_4(l)dlds$$

For $\hat{x}_1(t)$, it also follows that

$$\hat{x}_1(t) = x_1(t-\tau) + x_2(t-\tau)\tau + \int_{t-\tau}^{t}\int_{t-\tau}^{s} \hat{x}_3(l)dlds$$

It can be observed from Proposition 1 that the closed-loop system of the (3) with the controller $u(t) := K\hat{x}(t)$ remains stable. Thus without loss of generality and using Theorem 1, it can be easily deduced that $\hat{x}_i \to x_i$.

C. Nested saturation analysis

Observe that the controllers u_θ and u_ϕ are based in nested saturation functions. As previously mentioned the analysis is only presented for the longitudinal dynamics, as a similar procedure can be used for the lateral dynamic. Hence, the longitudinal dynamic it is described as

$$\begin{aligned} \ddot{x}(t) &\approx -g\theta_1(t) \\ \ddot{\theta}(t) &= u_\theta(t-\tau) \end{aligned}$$

where $u_\theta(t-\tau) = u(x_1(t-\tau), x_2(t-\tau), \theta_1(t-\tau), \theta_2(t-\tau))$.

Let us define the error $e_{\hat{\theta}} = \hat{\theta} - \theta$. Observe that from Theorem 1 : $\hat{\theta} \to \theta$. Thus we can consider that after a time $T_{\hat{\theta}}$, $e_{\hat{\theta}} << 1$, such that $|e_{\hat{\theta}}| \leq \delta_{\hat{\theta}}$ with $\delta_{\hat{\theta}} > 0$.

Propose the following control using the predicted states

$$u_\theta(t-\tau) := -\sigma_1(\hat{\theta}_2 + \varepsilon_2) \tag{31}$$

where $\sigma_i(s)$ is a saturation function such that $|\sigma_i(s)| \leq M_i$ and ε_i is a bounded function that will be defined later to prove convergence. In addition, $|\varepsilon_i| \leq M_{\varepsilon_i}$. We propose the following positive definite function $V_1(t) = \frac{1}{2}\theta_2^2(t)$, then $\dot{V}_1(t) = -\theta_2\sigma_1(\hat{\theta}_2 + \varepsilon_1)$.

If $e_{\hat{\theta}_2} \to 0$ then $\text{sign}(\hat{\theta}_2) = \text{sign}(\theta_2)$ and if $\left|\hat{\theta}_2(t)\right| > M_{\varepsilon_1}$, this implies that $\dot{V}_1(t) \leq 0$. Then after a time T_1 ; $\left|\hat{\theta}_2\right| \leq M_{\varepsilon_1}$. Choosing $M_1 \geq 2M_{\varepsilon_1}$, then $\forall\ t > T_1$

$$u_\theta(t-\tau) := -\hat{\theta}_2 - \varepsilon_1 \tag{32}$$

Define $z_1(t) \equiv \theta_1(t) + \theta_2(t)$, thus

$$\dot{z}_1(t) = \theta_2 - \hat{\theta}_2 - \varepsilon_1 \leq \delta_{\hat{\theta}_2} - \varepsilon_1$$

Define $\varepsilon_1 := \sigma_2(z_1(t) + \varepsilon_2)$, then $M_{\varepsilon_1} = M_2$. Propose $V_2(t) = \frac{1}{2}z_1^2(t)$, then

$$\dot{V}_2(t) \leq -z_1\left(\sigma_2(z_1(t) + \varepsilon_2) - \delta_{\hat{\theta}_2}\right)$$

Notice that $\delta_{\hat{\theta}_2}$ is arbitrarily small and $M_2 >> \delta_{\hat{\theta}_2}$, thus, if $|z_1| > M_{\varepsilon_2}$, this implies that $\dot{V}_2(t) \leq 0$ and then after a time T_2 ; $|z_1| \leq M_{\varepsilon_2}$. Choosing $M_2 \geq 2M_{\varepsilon_2}$, then $\forall\ t > T_2$

$$u_\theta(t-\tau) := -2\hat{\theta}_2 - \hat{\theta}_1 + e_{\hat{\theta}_2} + e_{\hat{\theta}_1} - \varepsilon_2 \tag{33}$$

Define $z_2(t) = z_1(t) + \theta_1(t) - \frac{x_2(t)}{g}$, then

$$\dot{z}_2(t) = -e_{\hat{\theta}_2} - \varepsilon_2 \leq \delta_{\hat{\theta}_2} - \varepsilon_2$$

Define $\varepsilon_2 := \sigma_3(z_2(t) + \varepsilon_3)$, then $M_{\varepsilon_2} = M_3$. Propose $V_3(t) = \frac{1}{2}z_2^2(t)$, then

$$\dot{V}_3(t) \leq -z_2\left(\sigma_3(z_2(t)\varepsilon_3) - \delta_{\hat{\theta}_2}\right)$$

Observe again that $\delta_{\hat{\theta}_2}$ is arbitrarily small and $M_3 >> \delta_{\hat{\theta}_2}$, thus, if $|z_2| > M_{\varepsilon_2}$, this implies that $\dot{V}_2(t) \leq 0$ and then after a time T_3 ; $|z_2| \leq M_{\varepsilon_3}$. Choosing $M_3 \geq 2M_{\varepsilon_3}$, then $\forall\ t > T_3$

$$u_\theta(t-\tau) = -3\hat{\theta}_2 - 3\hat{\theta}_1 + 2e_{\hat{\theta}_2} + 3e_{\hat{\theta}_1} + \frac{\hat{x}_2}{g} - \frac{e_{\hat{x}_2}}{g} - \varepsilon_3$$

Finally define $z_3(t) \equiv z_2(t) - 2\frac{x_2(t)}{g} + \theta_1 - \frac{x_1(t)}{g}$, then

$$\dot{z}_3(t) = -e_{\hat{\theta}_2} - \varepsilon_3 \leq \delta_{\hat{\theta}_2} - \varepsilon_3$$

Define $\varepsilon_3 := \sigma_4(z_3(t))$, then $M_{\varepsilon_3} = M_4$. Propose $V_4 = \frac{1}{2}z_3^2$ thus $\dot{V}_4 = -z_3(\sigma_4(z_3(t)) + \delta_{\hat{\theta}_2})$. Notice that $M_4 \gg \delta_{\hat{\theta}_2}$ and this implies that z_3 is bounded and decreases and then after a time T_4 the controller can be rewritten as

$$\begin{aligned} u_\theta(t-\tau) &= -4\hat{\theta}_2 - 6\hat{\theta}_1 + \frac{4\hat{x}_2}{g} + \frac{\hat{x}_1}{g} \\ &\quad +3e_{\hat{\theta}_2} + 6e_{\hat{\theta}_1} - \frac{4e_{\hat{x}_2}}{g} - \frac{e_{\hat{x}_1}}{g} \end{aligned}$$

From Proposition 1, $u_\theta(t-\tau)$ could be expressed as $u(t, \hat{\mathbf{x}})$ and in addition remember that $\hat{\mathbf{x_i}} \to x_i$ and this implies that $\delta_{(\hat{\theta}_i, \hat{x}_i)} \to 0$. Hence, the previous controller becomes

$$\begin{aligned} u_\theta(t) &= -4\hat{\theta}_2 - 6\hat{\theta}_1 + \frac{4\hat{x}_2}{g} + \frac{\hat{x}_1}{g} \\ &= \mathbf{K}\hat{\mathbf{x}}(t) \end{aligned}$$

where $K = [1/g \ \ 4/g \ \ -6 \ \ -4]$ and $\hat{x}^T = [\hat{x}_1 \ \ \hat{x}_2 \ \ \hat{\theta}_1 \ \ \hat{\theta}_2]$. The convergence of the states is proved by applying Theorem 1. Therefore, the control inputs for the longitudinal and lateral systems are

$$\begin{aligned} u_\phi(t) &:= -\sigma_{\phi_1}\left(\hat{\phi}_2(t) + \sigma_{\phi_2}\left(\varrho_1 + \sigma_{\phi_3}\left(\eta_1 + \sigma_{\phi_4}\left(\zeta_1\right)\right)\right)\right) \\ u_\theta(t) &:= -\sigma_{\theta_1}\left(\hat{\theta}_2(t) + \sigma_{\theta_2}\left(\varrho_2 + \sigma_{\theta_3}\left(\eta_2 + \sigma_{\theta_4}\left(\zeta_2\right)\right)\right)\right) \end{aligned}$$

where

$$\begin{aligned} \varrho_1 &:= \hat{\phi}_1(t) + \hat{\phi}_2(t) \\ \eta_1 &:= 2\hat{\phi}_1(t) + \hat{\phi}_2(t) + \frac{\hat{y}_2(t)}{g} \\ \zeta_1 &:= \hat{\phi}_2(t) + 3\hat{\phi}_1(t) + 3\frac{\hat{y}_2(t)}{g} + \frac{\hat{y}_1(t)}{g} \\ \varrho_2 &:= \hat{\theta}_1(t) + \hat{\theta}_2(t) \\ \eta_2 &:= 2\hat{\theta}_1(t) + \hat{\theta}_2(t) - \frac{\hat{x}_2(t)}{g} \\ \zeta_2 &:= \hat{\theta}_2 + 3\hat{\theta}_1(t) - 3\frac{\hat{x}_2(t)}{g} - \frac{\hat{x}_1(t)}{g} \end{aligned}$$

IV. Numerical validation

In this section we present preliminary simulation and emulation results aiming at a correct turning of our control law.

A. Simulation

For simulation purposes the nonlinear model (29) is used. First, the control law is validated for the ideal case when no input delays are present. The desired values are $x_{1d} = 10$, $y_{1d} = 5$ and $z_{1d} = 1$, and the initial conditions for all states are set to zero except $z_1(0) = 10$. Figure 1 shows the state responses. For clarity of presentation we only depict the positions (x, y, z) of the vehicle.

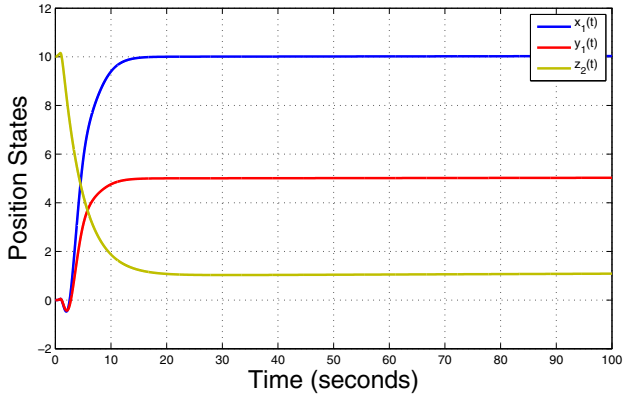

Fig. 1. States x_1, y_1, z_1 without delay in the input

Next, we introduce a delay in the measurement. Tests were made in order to find the critical values $h_1^*$and h_2^* of the delays h_1 and h_2. To do so, we set one delay to zero and increase gradually the other one, until instability is observed. It is found that $h_1^* = 0.09s$ and $h_2^* = 0.24$. See illustrative cases on Figures 2 and 3.

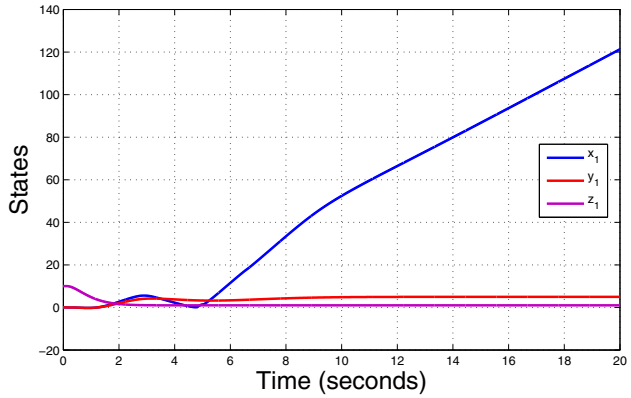

Fig. 2. States x_1, y_1, z_1 with delay $h_1 = 0.1$

When implementing our control-predictor scheme, delays were introduced in each of the 12 states of the nonlinear dynamical model. We introduced two delays values, $h_1 = 0.9s$ in the translational movement (x_1, x_2, y_1, y_2, z_1 and z_2), and $h_2 = 0.3s$ in the attitude (θ_1, θ_2, ϕ_1, ϕ_2, ψ_1 and ψ_2). In Figure 4 it can be appreciated that all the states still converge to the desired values even thought the values of the delay are bigger than the critical delays.

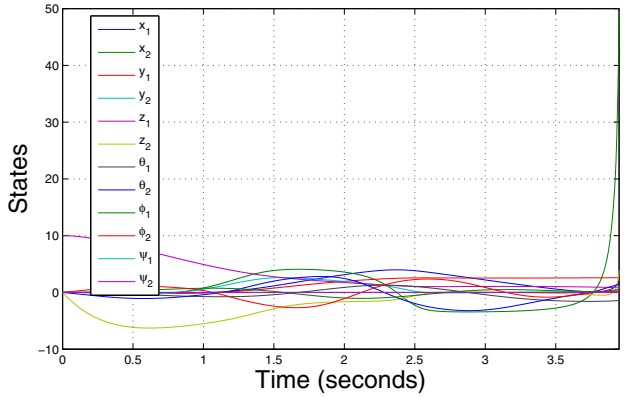

Fig. 3. States x_1, y_1, z_1 with delay $h_2 = 0.25$

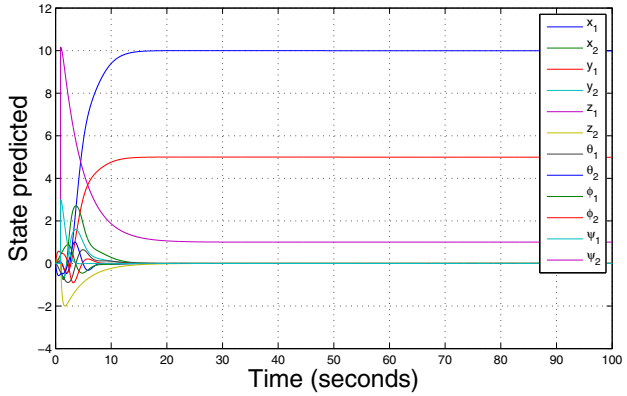

Fig. 4. System response with predictor and delay values $h_1 = 0.9$, $h_2 = 0.3$

B. Emulation

In real-time experiments the sensors measurements are usually noisy or inaccurate. These intrinsic anomalies degrade the behavior of the system, and inclusively destabilize it. In order to evaluate their impact in the closed-loop, we emulate noise and dropout data as described on Figure 5 in the system loop. The resulting system behavior is shown in Figure 6, which shows that the system still get to the desired values and that the degradation of the performance is quite acceptable.

V. Experimental Results

The proposed predictor control scheme is also validated with real-data. The objective of the flight test is to follow a rectangle trajectory in automatic mode without delay. The collected data are delayed in order to validate our predictor control scheme. The height (z) is imposed to be constant. In the following figures, and due paper length limitations, only the position in the horizontal plane is presented (longitudinal and lateral dynamics).

First, the measurement delays h_1 and h_2 are set to 15 sampling periods. The predictor responses (Figures 7 and 8) show that the real and predicted values of the states are similar and the error goes to zero. Figure 7 depicts the responses for x_1, y_1, $\hat{x}_1$ and $\hat{y}_1$.

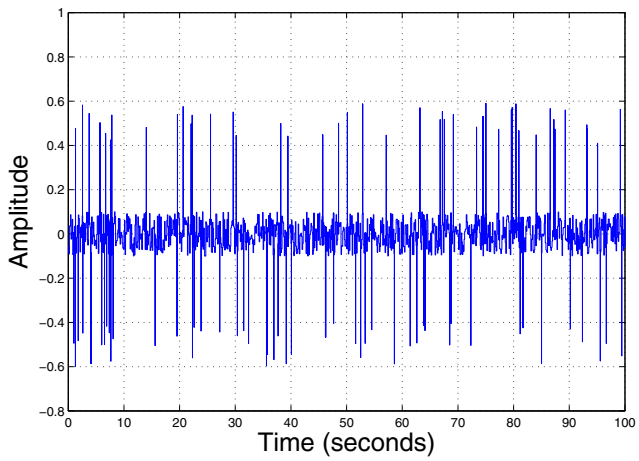

Fig. 5. Noise and dropout data

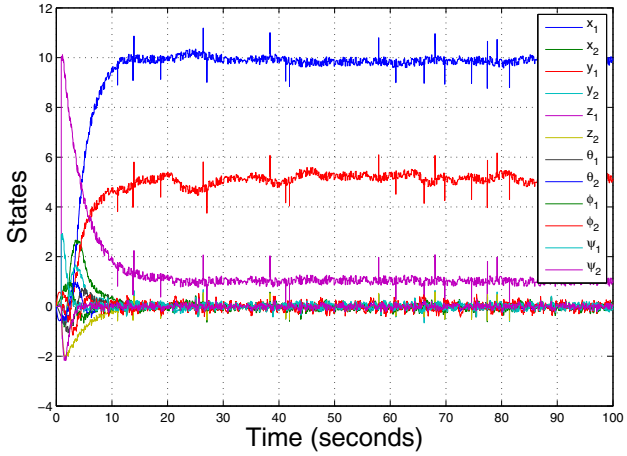

Fig. 6. System response with predictor and delay values h_1 = 0.9, h_2 = 0.3 adding noise and dropout data

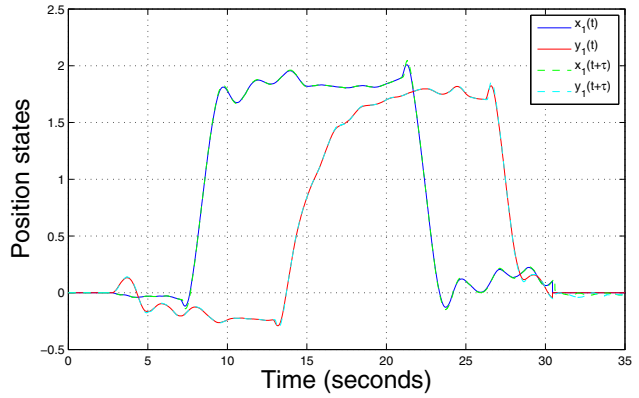

Fig. 7. x, y responses. The dotted line represents $\hat{x}$, $\hat{y}$

Next the delays h_1 and h_2 are increased to 40 sampling periods. The horizontal position responses are depicted in Figure 9. Notice that even if the delay is big, the predictor scheme is able to predict correctly the state variables values.

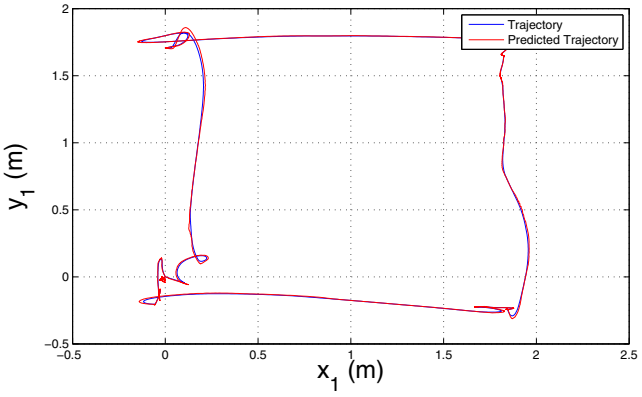

Fig. 8. $(x_1(t),y_1(t))$ plane trajectory vs $(\hat{x}_1(t),\hat{y}_1(t))$ plane trajectory

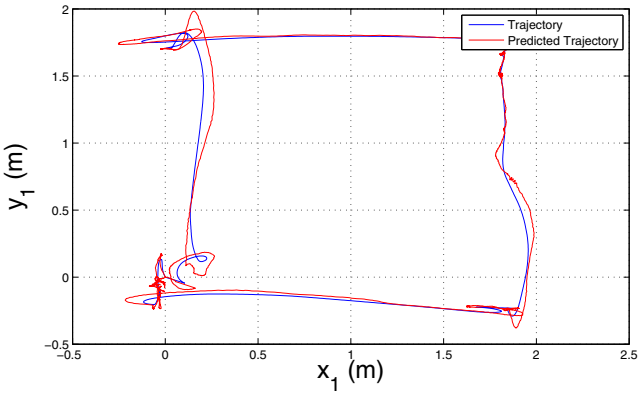

Fig. 9. $(x_1(t),y_1(t))$ plane trajectory vs $(\hat{x}_1(t),\hat{y}_1(t))$ plane trajectory

Finally we follow a rectangular trajectory, using measurements obtained from a GPS sensor, model $6s - lea$ of the brand $ublox$, that provides measures every $200ms$. The position data is delayed 9 sampling periods while the velocity data 3 sampling periods. Notice in Figures 10 - 13 the obtained results. In Figure 10 the x displacement is presented, in order to better illustrate the result a zoom of this figure is realized. Figure 10 illustrates the delayed measure (red dotted line), the state (blue solid line) and the predicted state (black dashed line). Data are depicted in the coordinate system ECEF.

In Figures 12 and 13 the velocity response in the x axis is presented. Figure 13 is a zoom-in of Figure 12. Recall that for aerial vehicles the velocity responses need to be very fast in order to stabilize the vehicle. Delaying this state 9 sampling periods as the position gives an unstable system, therefore it was delayed only by 3 sampling periods. Recall also that the sampling period is 200 ms then the measure for velocity has a delay of 600 ms. We consider that this delay is big for the velocity and is adequate for our purposes.

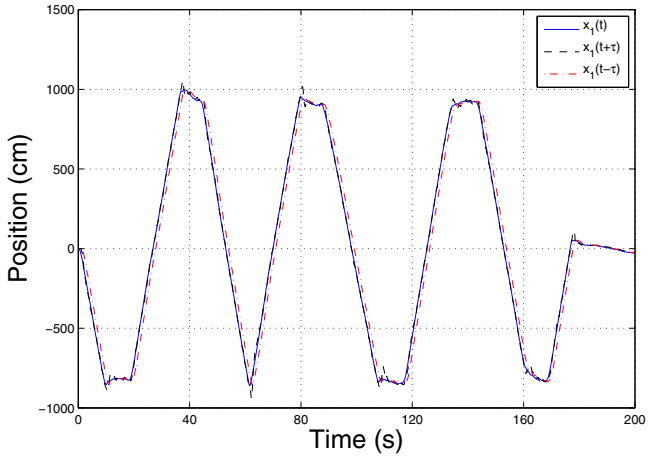

Fig. 10. State response in the x axis in the coordinate system ECEF

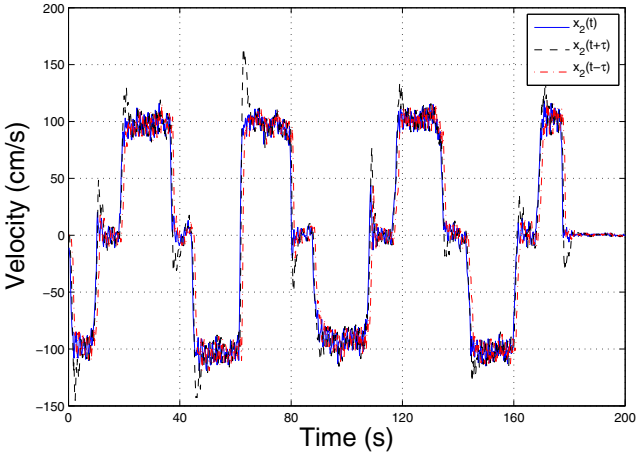

Fig. 12. Velocity response in the x direction of the coordinate system ECEF

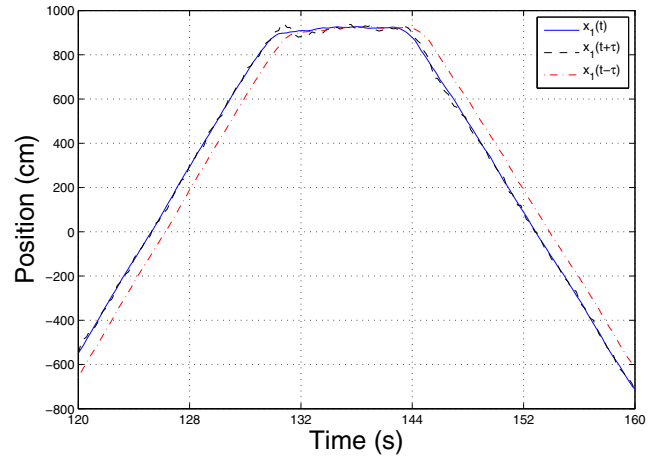

Fig. 11. Zoom-in of Figure 10

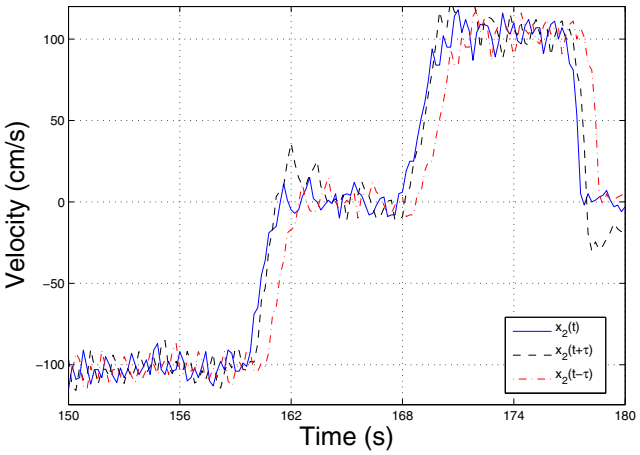

Fig. 13. Zoom-in of Figure 12

VI. Conclusion & Future work

A predictor-control scheme based on the Fundamental Theorem of Calculus is proposed in this paper. Exponential stability of the closed-loop system is proved using the Backstepping approach for a chain of n integrators in cascade. The stabilization of a quadrotor vehicle is carried out by combining a nonlinear algorithm based on nested saturation with the above results. Several simulations results validate the proposed scheme. In particular, noise and dropout data are introduced to emulate a practical situation. Real-data experiments show that the proposed predictor-control scheme is an effective control strategy of quadrotor aerial vehicles. Future work include experimental on-line flight tests and the development of control laws aiming at improving the robustness of the predictor scheme.

References

[1] K. Lee, H. Kim, J. Park, Y. Choi Hovering Control of a Quadrotor International Conference on Control, Automation and Systems Oct. 17-21, 2012 in ICC, Jeju Island, Korea.

[2] H. Voos Nonlinear Control of a Quadrotor Micro-UAV using Feedback-Linearization Proceedings of the 2009 IEEE International Conference on Mechatronics. Malaga, Spain, April 2009

[3] P. Pounds, R. Mahony, P. Corke Modelling and control of a large quadrotor robot Control Engineering Practice 18 691-699. 2010.

[4] T. Madani, A. Benallegue Backstepping Control for a Quadrotor Helicopter International Conference on Intelligent Robots and Systems. October 9 - 15, 2006, Beijing, China.

[5] D. Mellinger, N. Michael, V. Kumar Trajectory generation and control for precise aggressive maneuvers with quadrotors International The International Journal of Robotics Research 31(5) 664-674.

[6] A. Chan, S. Tan, C. Kwek Sensor data fusion for attitude stabilization in a low cost Quadrotor system International Symposium on Consumer Electronics 2011

[7] O. Smith, Closer control of loops with dead time, Chemical Engineering progress, 53(5), pp. 217-219 1957.

[8] A. Manitius, A. Olbrot Finite spectrum asigment problems for systems with delays, IEEE Transactions on Automatic Control, 24(4), pp. 541-553, 1979.

[9] K. Astrom, C. Hang, B. Lim Ã new smith predictor for controlling a process with integrator and a long dead-time, IEEE Transactions on Automatic Control vol. 39, pp.343-345 Feb. 1994.

[10] Z. Palmor, Time-delay compensation Smith predictor and it's modifications, The control handbook, pp. 224-237 Ed. Bca Raton, Fl :CRC, 1996

[11] A. Manitius, A. Olbrot Finite spectrum asigment problems for systems with delays, IEEE Transactions on Automatic Control, 24(4), pp. 541-553, 1979.

[12] S. Mondie, M. Dambrine, O. Santos Aproximation of control laws with distributed delays : A necessary condition for stability, presented at the IFAC Fonf, Syste, Structure, Control, Prague Aug. 2001.

[13] V. Assch, M. Dambine, J. Lafay, J. Richard Some problesm arising in the implementation of distributed delays control laws, presented at the 38th IEEE Conf. Decision Control Phoenix, AZ, Dec. 1999.

[14] D. Yue, Q. Han Delayed feedbac control of uncertain systems with tme varying input delay, Automatica 41(2), pp. 233-240 2005.

[15] J. Nomey-Rico, E. Camacho Dead time compensators : A survey, Control engineering practice 16(4), pp. 407-428 2008.

[16] J. Guzman, P. Garcia, I. Hagglund, S. Dormido, P. Albertos, M. BereguelInteractive tools for analysis of time-delay systems with dead time compensators, Control engineering practice, 16(7) pp. 824-835 2008

[17] M. Krstic Delay Compensation for nonlinear, adaptive and PDE systems Birkhauser, Boston, 2009.

[18] R. Lozano, P. Castillo, P. Garcia, A. Dzul Robust prediction-based control for unstable delay systems : Application to the yaw control of a mini-helicopter, Automatica 40(4), pp. 603-612 Aug. 2004.

[19] J. Ordaz, S. Salazar, S. Mondié, H. Romero, R. Lozano Predictor-based Position Control of a Quad-rotor with Delay in GPS and Vision Measurements, Springer, August, 2012

[20] P. Castillo, R. Lozano, A. Dzul Modelling and Control of Mini-Flying Machines, Springer